Charge and polarization distributions at the 90° domain wall in barium titanate ferroelectric

Qingsong Zhang and William A. Goddard III[a)]
Materials and Processes Simulation Center (MC 139-74), 1200 E. California Blvd., California Institute of Technology, Pasadena, California 91125

(Received 30 June 2006; accepted 15 September 2006; published online 31 October 2006)

The authors use the PQEq force field based on quantum mechanics studies to provide a first-principles description of the 90° domain wall in barium titanate. Using periodic cells with lengths of up to 74 nm (5120 atoms), the authors find that the domain wall thickness is 21 nm in which the polarization switches over a 5 nm central layer surrounded by two transition layers each 8 nm wide. The central 5 nm layer consists of a 2 nm sublayer with overshooting polarizations and a 3 nm sublayer with reversed polarization. This structure explains the discrepancies in previous analyses, which have suggested domain walls ranging from 100 nm to 1 nm. These results should be of particular importance in developing nanoscale ferroelectric devices. © *2006 American Institute of Physics*. [DOI: 10.1063/1.2374676]

Ferroelectric (FE) materials exhibit domains over which the atom displacements lead to a net dipole polarization in one direction alternating with domains with the polarization in another direction. In the tetragonal phase the polarization changes by 180° or 90°. These domains can be switched by applying external electric fields or stresses, leading to broad applications in transducers, actuators, capacitors, and memories. The nature of the domain boundary and the mechanism by which the domains switch determine the performance properties. In addition they are probably important in determining the mechanical and electrical failures associated with aging. In order to understand the origin of these phenomena and to design materials with improved performance, particularly as devices are miniaturized into the nanoscale, it would be most useful to have a detailed understanding of the structural and dynamic properties of the domain boundaries. There are some data from both experiment and theory on the 180° domain boundary; however, much less is known about the 90° domain walls observed in the perovskite tetragonal phase.

For example, experimental data on the width of $BaTiO_3$ 90° domain walls show substantial discrepancies.

(1) The width was estimated around 400 nm from polarized light microscopy (PLM).[1]
(2) Later the width was found to be 4–20 nm from transmission electron microscopy (TEM),[2–4] high resolution TEM (HRTEM),[5] and x-ray powder diffraction (XRPD).[6]
(3) But a surprisingly small thickness of 1.5–2.5 nm was obtained from electron holography (EH) by measuring the polarization induced phase shift.[7]

A Landau-Ginzburg-Devonshire (LGD)-type of phenomenological theory[8–10] has long been applied to study the $BaTiO_3$ 90° domain wall.[11–15] In LGD, the free energy is expressed as a function of such physical properties as strains and/or polarizations (called order parameters). To predict qualitatively the individual material properties a reduced form of this theory is usually applied with the various coefficients in the free energy expression determined by comparing to either experiment or quantum mechanics (QM) calculations. In the LGD theory the finite width of domain wall is attributed to the energy penalty caused by certain order parameter gradients. By analyzing strain gradients Kittel[11] estimated the wall width as 100 nm (wall energy of $\sim 100\ \mathrm{ergs/cm^2}$). By using the polarization gradient Zhirnov[12] reported a wall width between 5 and 10 mm (wall energy of $2-4\ \mathrm{ergs/cm^2}$). Including high-order polarization terms in the Zhirnov theory[12] Bulaevskii[13] found a much smaller thickness of 1.1 nm (wall energy of $3.4\ \mathrm{ergs/cm^2}$). The LGD theory was further improved with symmetry requirements by Cao and Cross[14] and with external applied mechanical load and electric field by Shu and Bhattacharya.[15]

Summarizing, various experiments and theories predict three categories of domain wall widths: broad[1,11] (100–400 nm), medium[2–6] (5–20 nm), and narrow,[7,13] (1.5–2.5 nm).

Quantum mechanics calculations[16,17] provide a powerful approach to attain a deeper theoretical understanding of domain walls. Meyer and Vanderbilt[18] studied $PbTiO_3$ 90° domain walls using density functional theory (DFT) and found a surprisingly narrow width of 0.45–0.55 nm. However, these QM were limited to quite small cells (~70 atoms). Thus the Meyer and Vanderbilt study imposed a domain wall distance of 0.8–2.0 nm (cell sizes of 30–70 atoms), much smaller than most experimental estimates of the separation between two domain walls! For these small cells the QM studies for the $BaTiO_3$ tetragonal phase structure found that the displacive mode[19,20] (leading to Ti atoms to the corners of octahedra) is dynamically unstable.

Herein, we present a first-principles study of the 90° domain wall for $BaTiO_3$, considering unit cells with up to 74 nm (5120 atoms), which we show as large enough to describe converged 90° domain wall systems. Then we address the fundamental reasons for the discrepancies between previous theoretical and experimental results.

Our QM calculations[21] for of $BiTiO_3$ considered cubic unit cells with 8 f.u. and showed that the eight independent Ti distort toward octahedral faces in such a way that the full crystal has antiferroelectric (AFE) coupling in the x, y, and z

[a)]Author to whom correspondence should be addressed; FAX: 626-585-0918; electronic mail: wag@wag.caltech.edu

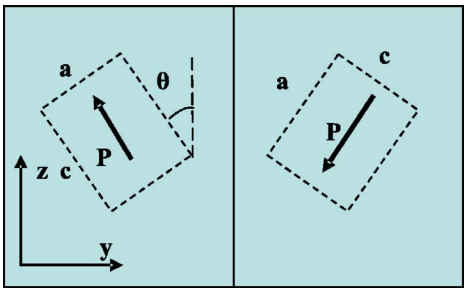

FIG. 1. (Color online) Supercell geometries used in the periodical boundary condition calculations. The polarization is along $[0\bar{1}1]$ on the left and $[0\bar{1}\bar{1}]$ on the right in the supercell coordinate system.

directions. This cubic unit cell of eight perovskite unit cells (space group I-43m) has zero net moment in all directions. In turn the tetragonal phase has a fundamental tetragonal unit cell of eight perovskite unit cells (space group I4cm), with AFE coupling in the x and y directions, but FE coupling in the z direction. The QM shows that this FE-AFE model is dynamically stable.

Based on the QM calculations for the cubic, tetragonal, orthorhombic, and rhombohedral structures as a function of pressure, we developed the PQEq force field[21] in which the charge of each atom is described as a superposition of a Gaussian shaped positive charge and a Gaussian shaped negative charge. The charges can transfer from atom to atom as in the charge equilibration (QEq) method[22] and the centers of the positive and negative centers can be displaced independently. We also include two-body Morse functions to describe short range Pauli repulsion. All the parameters are fitted to the energies and charges from the QM calculation

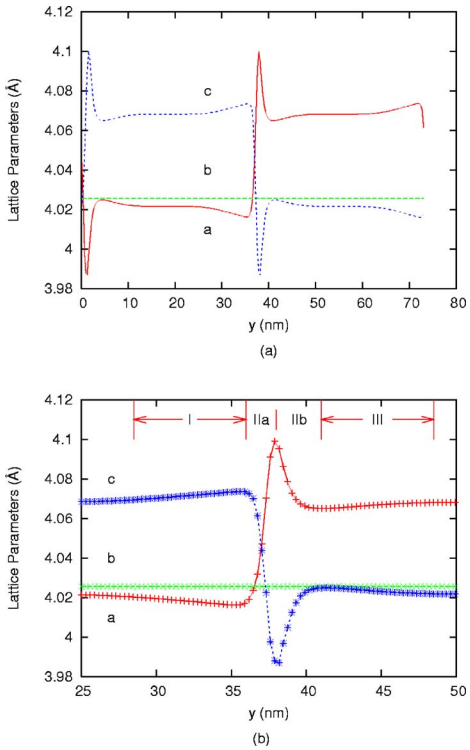

FIG. 2. (Color online) Unit cell distortions over the $BaTiO_3$ 90° domain wall. The polarization is along $[0\bar{1}1]$ on the left and $[0\bar{1}\bar{1}]$ on the right in the supercell coordinate system. (b) expands the domain wall region from (a). The relative magnitudes of (a) and (c) switch across the 90° domain wall, leading to an 89.4° rotation of lattice orientation.

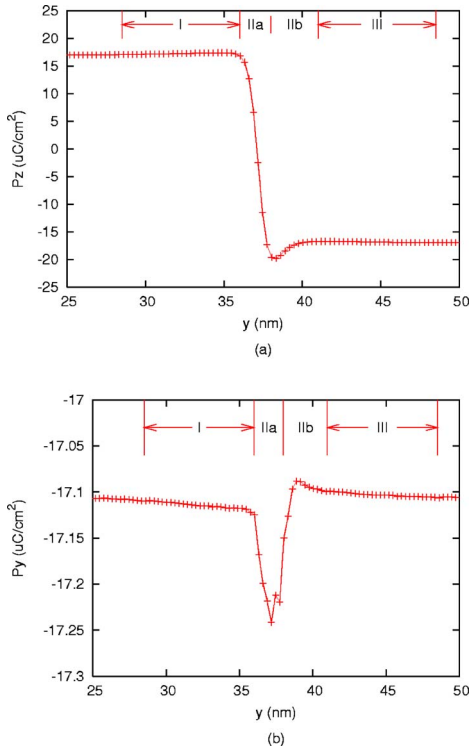

FIG. 3. (Color online) Polarization across the $BaTiO_3$ 90° domain wall. (b) and (c) show the Pz and Py components in the amplified domain wall region from (a). Pz overshoots and then relaxes in the central layer. Py increases its amplitude in the central layer.

(no experimental parameters are used). We find that P-QEq leads to the same FE-AFE structures and relative energies as the QM. All calculations use analytic forces based on this first-principles PQEq force field[21] optimized to fit QM calculations on $BaTiO_3$.

To determine the domain wall structures and energies, we used a supercell containing two 90° domain walls (Fig. 1), with dimensions of $2a$, $Nc/(4\sqrt{1+(c/a)^2})$, and $2a\sqrt{1+(c/a)^2}$ in the x, y, and z directions, respectively. This supercell contains 5120 atoms ($N=1024$) with a distance of $L=37$ nm separating the two walls. The other two dimensions are 0.81 and 1.14 nm. We minimized fully (all cell parameters and fractional coordinates) this initial structure using periodic boundary conditions.

We find that the domain wall transition region (Fig. 2) is 21 nm, consisting of a central 5 nm fast transition layer (layer II) and two adjacent 8 nm relaxation layers (layers I and III). The central transition layer consists of a 2 nm sublayer (sublayer IIa) displaying overshooting switches in polarization and lattice parameter (Fig. 3) and a 3 nm sublayer (sublayer IIb) with smaller switches in polarization.

The polarization switches abruptly due to the low energy of the antiparallel polarization state while the strain switches smoothly because of the lattice match conditions required between neighboring cells. The competition of these two effects leads to a layered structure responsible for a diffraction contrast of 5 nm (sharp limit) to 20 nm wide in agreement with diffraction-based experiments[2–6] (TEM, HRTEM, and XRPD), and polarization contrast of 2 nm wide, in agreement with polarization-based techniques[7] (EH). We suspect that the extremely large 400 nm width observed by PLM (Ref. 1) is caused by small domain wall tilting (which our

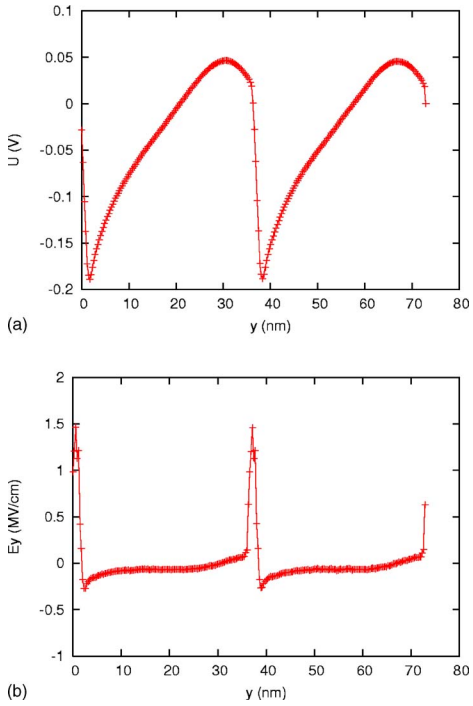

FIG. 4. (Color online) Electric potential (a) and electric field distribution (b). We find a large electric field (1.5 MV/cm) at the central layer (2 nm wide) of the domain wall, leading to 0.23 V electric potential change across the wall.

calculations suggest as 2.3°) in the 10 μm thick sample used in the experiment.

LGD calculations predict a wide wall (~100 nm) when strain and its gradient were treated as the order parameters[11] while a medium wall (2–4 nm) was obtained when polarization and its gradient were used.[12] LGD led to a narrower wall (1.1 nm) when high-order polarization terms were included.[13] Without the lattice match conditions the various LGD theories predicted[12–15] synchronized relaxations of strain and polarization.

The normal polarization component (P_y) has a small magnitude increase of 0.14 μC/cm^2 at the wall center (Fig. 3). This contrast with the decrease of 1.5 μC/cm^2 in $PbTiO_3$.[18] We believe that the reason is that the tetragonal phase of $BaTiO_3$ has local displacements along {111},[23] while $PbTiO_3$ has local displacements along {001}. At the domain wall center, the $BaTiO_3$ has a structure similar to its orthogonal phase, leading to larger polarization components along {011}.

The electric potential (U) induced by polarization is governed by Poisson's equation. $\nabla^2 U(r) = -\rho(r)$, where ρ is the polarization charge density given by $\rho(r) = -\text{div}\,\mathbf{P}(r)$. Due to the quasi-one-dimensional configuration, this equation reduces further to $(d^2/dy^2)U(y) = (d/dy)P_y(y)$, with $U(y) = U(y+2L)$. Solving this equation, we find that the maximum electric field is 1.5 MV/cm (Fig. 4) across the domain wall, leading to 0.23 V electric potential difference between the two sides of the wall. This can be compared to the value of 0.18 V predicted in $PbTiO_3$ from DFT calculations.[18]

We calculate a 90° domain wall energy of 29 ergs/cm^2, which lies between the LGD prediction assuming a pure strain gradient[11] (~100 ergs/cm^2) and the LGD prediction[12,13] assuming a pure polarization gradient (2–4 ergs/cm^2).

We also studied how the domain walls would be affected by reducing L from 37 nm (N=5120) to 18, 9, and 4.5 nm (N=2560, 1280, and 640, respectively). For L=9 and 4.5 nm, the strain fields of the domain walls overlap each other, leading to an unstable structure which transforms to a single orthorhombic domain. Thus the 90° domains are not stable below a critical width, L_{crit}, which lies between 9 and 18 nm. These results suggest that the 90° domain walls constitute the natural nucleation sites for the tetragonal to orthogonal transition, in agreement with the suggestion by Cao and Cross.[14]

To evaluate the long-range electrostatic energy exactly, we use Ewald summation,[24] which consists of short-range real-space terms and long-range reciprocal-space terms. The long-range terms play a critical role in determining the domain wall structure. We find that truncation of these long-range terms increases the width of the domain wall, and that removing all long-range terms leads to an unstable wall structure that transforms into the orthorhombic phase. This result shows that it is essential to include the long-range effects in studying ferroelectrics. Such improvement has recently been implemented[15] in the LGD theory.

Summarizing, we determined the structure and properties of $BaTiO_3$ 90° domain wall using the PQEq first-principles force field. The layered wall structure found in this study explains the discrepancies of domain wall widths and wall energies in previous experimental and theoretical studies. We find that long-range interactions are essential to stabilize the layered domain wall structure.

This work was initiated with funding by the Army Research Office (MURI-DAAD19-01-1-0517) and by the National Science Foundation (MRSEC-CSEM-DMR0080065) and completed with funding from DARPA-PROM through the Office of Naval Research (N00014-02-1-0839). The MSC computational facilities used in these calculations were provided by grants from DURIP-ARO, DURIP-ONR, and NSF (MRI).

[1] E. A. Little, Phys. Rev. **98**, 978 (1955).
[2] M. Tanaka and G. Honjo, J. Phys. Soc. Jpn. **19**, 954 (1964).
[3] S. I. Yakunin, V. V. Shakmano, G. V. Spivak, and N. V. Vasil'eva, Fiz. Tverd. Tela (S.-Peterburg) **14**, 373 (1972).
[4] M. D. Dennis and R. C. Bradt, J. Appl. Phys. **45**, 1931 (1974).
[5] F. Tsai, V. Khiznichenko, and J. M. Cowley, Ultramicroscopy **45**, 55 (1992).
[6] N. Floquet and C. Valot, Ferroelectrics **234**, 107 (1999).
[7] X. Zhang, T. Hashimoto, and D. C. Joy, Appl. Phys. Lett. **60**, 784 (1992).
[8] A. F. Devonshire, Philos. Mag. **42**, 1065 (1951).
[9] A. F. Devonshire, Philos. Mag. **40**, 1040 (1949).
[10] A. F. Devonshire, Adv. Phys. **3**, 85 (1954).
[11] C. Kittel, Solid State Commun. **10**, 119 (1972).
[12] V. A. Zhirnov, Sov. Phys. JETP **8**, 822 (1959).
[13] L. N. Bulaevskii, Sov. Phys. Solid State **5**, 2329 (1964).
[14] W. W. Cao and L. E. Cross, Phys. Rev. B **44**, 5 (1991).
[15] Y. C. Shu and K. Bhattacharya, Philos. Mag. B **81**, 2021 (2001).
[16] W. Kohn and L. J. Sham, Phys. Rev. **140**, 1133 (1965).
[17] P. Hohenberg and W. Kohn, Phys. Rev. **136**, 864 (1964).
[18] B. Meyer and D. Vanderbilt, Phys. Rev. B **65**, 104111 (2002).
[19] W. Cochran, Adv. Phys. **9**, 387 (1960).
[20] W. Cochran, Phys. Rev. Lett. **3**, 412 (1959).
[21] Q. Zhang, Ph.D. thesis, Materials Science, Caltech, 2004; Q. Zhang, T. Cagin, and W. A. Goddard, III, Proc. Natl. Acad. Sci. U.S.A. **103**, 14695 (2006).
[22] A. K. Rappé and W. A. Goddard III, J. Phys. Chem. **95**, 3358 (1991).
[23] B. Ravel, E. A. Stern, R. I. Vedrinskii, and V. Kraizman, Ferroelectrics **206**, 407 (1998).
[24] P. Ewald, Ann. Phys. **64**, 253 (1921).